Applied Surface Science 638 (2023) 158074

Contents lists available at ScienceDirect

Applied Surface Science

journal homepage: www.elsevier.com/locate/apsusc

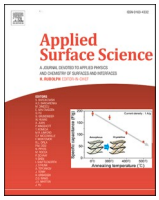

Full Length Article

Quantification of coverage, uniformity and residues for CVD monolayer graphene transfer process based on image analysis

Kevin Ballestas [a], Juan Diego Zapata [b], Daniel Ramírez [a,*]

[a] Centro de Investigación, Innovación y Desarrollo de Materiales (CIDEMAT), Faculty of Engineering, Universidad de Antioquia, Calle 70 # 52-21, Medellín, Colombia
[b] Faculty of Engineering, Universidad de Antioquia, Calle 70 # 52-21, Medellín, Colombia

ARTICLE INFO

Keywords:
CVD
Monolayer graphene
Microscopy images
Image analysis
MATLAB

ABSTRACT

The use of CVD-grown graphene requires a transfer method to transport this material from the metal foil on top of which it is grown onto a target substrate. In many cases this transfer changes its properties, leading to variations from one zone of the target substrate to another. Here we present a simple semi-automatic method for a quantitative study of the coverage, uniformity and residues of graphene transferred onto Si/SiO_2 substrates whose operation is not dependent on costly equipment, making it low-cost oriented. The method can be extrapolated to different target substrates, e.g., ITO-coated glass, and serves as an evaluation tool for graphene transfer processes. This is achieved by calculating a figure of merit, based on 2 proposed quantitative parameters (accounting for the coverage and the uniformity of the transferred graphene), while simultaneously determining the residues left by the transfer substrate using MATLAB-based image analysis of optical microscopy images. To corroborate the proposed method, a comparison between polydimethylsiloxane (PDMS), thermal release tape- (TRT) and polymethylmethacrylate- (PMMA) assisted transfer processes is performed, demonstrating that the methodology is valid for all cases. Coverages over 80 % are obtained, being in good agreement with results from the same transfer processes studied via Raman mapping.

1. Introduction

Since its discovery in 2004 [1], graphene has been extensively investigated due to its extraordinary electrical, optical and mechanical properties [2–4]. This has allowed graphene to be used in many applications across several fields and devices, including high-speed electronics, transistors, supercapacitors, energy storage, solar cells, sensors, CO_2 absorption, Erbium-doped fibre lasers and optical modulators [5–11]. Most of these applications rely on the widely used bottom-up method for the fabrication of graphene based on chemical vapor deposition (CVD) introduced in 2006 [12], which has allowed this material to be commercially available mainly in the form of monolayer graphene (MLG) or few-layer graphene (FLG) grown on top of metal substrates, being copper the most commonly used for this purpose. Consequently, in many scenarios where graphene is going to be employed, a transfer process that allows its transport from the metal substrate, on top of which it has been previously grown, to a target substrate is required. Many transfer processes have been reported in the literature, most of which employ a polymeric carrier substrate that assists the transport of graphene to the target substrate [13]. Methods using polymethylmethacrylate (PMMA) [14–17] or thermal release tape (TRT) [18–20] as a carrier substrate have been extensively used, and alternative approaches have also been reported, namely stamping transfer methods using polydimethylsiloxane (PDMS) [21–23] as carrier substrate and etching free methods using polymers to mechanically transfer graphene [24,25].

Following the transfer process, usually a characterization is required to assess the features of the as-transferred graphene on the target substrate. This has been typically done via Raman Spectroscopy, Atomic Force Microscopy (AFM), Scanning Electron Microscopy (SEM), Photoluminescence Spectroscopy and Raman Mapping [26–30], with the latter allowing for a thorough characterization of graphene regarding

Abbreviations: CVD, chemical vapor deposition; MLG, monolayer graphene; FLG, few layer graphene; PDMS, polydimethylsiloxane; TRT, thermal release tape; PMMA, polymethylmethacrylate; AFM, atomic force microscopy; SEM, scanning electron microscopy; EDS, energy-dispersive X-ray spectroscopy; ATR-FTIR, Attenuated Total Reflectance Fourier transform Infrared Spectroscopy, FoM, Figure of Merit; NMG, Not Monolayer Graphene; PET, polyethylene terephthalate; DI, deionized; FWHM, Full Width at Half Maximum; 0D, zero-dimensional; 1D, one-dimensional.

* Corresponding author.
E-mail address: estiben.ramirez@udea.edu.co (D. Ramírez).

https://doi.org/10.1016/j.apsusc.2023.158074
Received 31 May 2023; Received in revised form 13 July 2023; Accepted 18 July 2023
Available online 20 July 2023

number of layers, presence of defects, coverage and uniformity [26]. Additional techniques enabling a more macroscopic characterization have also been introduced in the literature, namely Van der Pauw measurements, which identify non-uniformities in graphene caused by unintended doping [28], and combined optical and sheet resistance measurements, which reveal macroscopic differences in electrical properties of graphene [27,29,30]. However, the aforementioned techniques pose a challenge as they require equipment that might not be available in many laboratories, e.g., Raman mapping cannot be performed in many facilities. For this reason, efforts towards an easier characterization of transferred graphene using computer-based strategies have been recently carried out. For instance, image processing can be combined with micro-Raman measurements to identify the thickness of transferred graphene from optical microscopy images [31]. More recently, deep learning and 3D deep learning combining optical RGB images and hyperspectral reflection images have been employed to segmentate and identify the thickness of graphene and MoS_2 flakes in optical microscopy images [32,33]. These strategies aim to characterize transferred graphene in a fast and automated manner, which would be highly valuable for quality control of industrial-scale fabrication processes of this material. Nonetheless, employing low-cost equipment for easily characterizing transferred graphene remains a challenge for its further insertion in the market.

Following this effort towards low-cost and industrial-scale compatible graphene characterization processes, we present a simple semi-automatic method for a quantitative and representative study of the coverage, uniformity and residues of graphene transferred onto Si/SiO_2 substrates which can be extrapolated to different target substrates and serves as an evaluation tool for graphene transfer processes. Combining MATLAB-based image analysis with optical microscopy images, a simple and readily measurable figure of merit (FoM) representative of the coverage and uniformity of transferred graphene is calculated based on 2 quantitative parameters proposed by the authors. Furthermore, a quantification of the residues left during the transfer process is performed using the same principle. The proposed parameters gauge three different features of the transferred graphene: the area of the target substrate that was effectively covered by graphene (coverage), the uniformity of the graphene regarding the presence of individual areas that were not effectively covered (uniformity) and the area of the target substrate that is covered with residues left from the transfer substrate used in the process (residues). The parameters were determined from mere optical microscopy images and no expensive equipment was used for their calculation, thus showing the ease of use of the method and its low-cost and industry-compatible operation. In addition, to corroborate the method, a direct comparison of PDMS-, TRT- and PMMA-assisted transfer processes is made, from which it is clearly and quantitatively indicated, based on the defined parameters, that the better results are obtained with the TRT-assisted transfer method while all the processes yield a coverage above 80 %. Additional characterization techniques including SEM, Energy-dispersive X-ray Spectroscopy (EDS), and Micro-Raman and Raman mapping were employed to verify the validity of the method.

2. Materials and methods

2.1. Materials

PDMS Gel-Pak DGL-X45 with a thickness of 6.5 mil (152.4 μm) used as a transfer substrate was acquired from Delphon. The TRT used for the transfer processes was acquired from Graphene Supermarket. Single layer graphene grown by CVD on Cu foil was purchased from 2D semiconductors. ITO-coated (Indium Tin Oxide) glass was purchased from Naranjo substrates.

2.2. PDMS- and TRT-assisted transfer methods

Graphene on Cu foil (only one side of the foil has graphene on top of it) is put in direct contact with the carrier substrate (PDMS or TRT) and a pressure of 0.2 MPa is applied for 30 min by using a load of known weight and controlling the application area with a glass substrate with customized dimensions. This allows the carrier substrate to adhere to the graphene/copper system. The carrier/graphene/copper system is taken to an etching solution (1 M ammonium persulfate solution) so that the copper is in contact with the solution and the foil floats on top of it, as schematized in Scheme 1. It is worth noting that it is not necessary to remove the graphene from the side of the copper foil that is in direct contact with the etching solution since graphene is only deposited in the other side. After 3 h, the copper foil is completely etched by the solution. The carrier/graphene system is then removed from the solution and rinsed with deionized (DI) water. Afterwards, it is dried with a flow of nitrogen. The system is then put in contact with the target substrate so that the graphene comes in contact with the substrate. A 0.5 MPa pressure is applied for 1 h and the carrier/graphene/target system is heated to 100 °C in a hot plate for 6 min. Finally, the carrier substrate is mechanically removed.

2.3. PMMA-assisted transfer method

Shortly, as reported elsewhere [34], a thin layer of PMMA was spin coated on top of a copper foil with CVD-grown graphene on it. The spin coating program was set at 3000 rpm, 1000 rpm/s for 60 s using a solution of PMMA in Anisole. Thereafter, an etching process with 1 M ammonium persulfate solution was done as described for the PDMS- and TRT-assisted transfer methods. This leaves a system of PMMA/graphene that was carefully rinsed with DI water and then scooped up using the target substrate. Then the PMMA/graphene/target system is heated at 100 °C for 1 h on a hot plate. Subsequently, the system is submerged in a chlorobenzene solution at 100 °C for 5 h to remove the PMMA layer. Finally, the graphene/target system is rinsed with isopropanol and dried with a flow of dried air.

2.4. Characterization

Micro Raman spectroscopy measurements, which were employed for characterizing CVD-grown and transferred graphene, were performed with a Horiba Yvon equipment, using a 632.81 nm laser (1.96 eV energy). Optical microscopy images, which were employed for performing image analysis of transferred graphene as well as assessing the working principle of PDMS as carrier substrate, were taken with a Leica DM750P microscope. Scanning Electron Microscopy images (SEM) and energy-dispersive X-ray spectroscopy (EDS) analyses, which were used for characterizing CVD-grown graphene on copper foil, were carried out with a JEOL-JSM 6490LV equipment. Attenuated Total Reflectance Fourier transform Infra-red Spectroscopy (ATR-FTIR), which was used for studying the working principle and structure of PDMS and TRT as carrier substrates, was performed with a NICOLET 6700 equipment.

2.5. Image analysis

Analysis of the optical microscopy images (taken at 500x zoom) was performed using a code designed by the authors in MATLAB using predefined functions in the Image Processing and Computer Vision toolboxes. Shortly, the code performs a binarization of each image to analyze, from which a black and white image is obtained, where white pixels correspond to zones covered with graphene and black pixels to zones that are not covered. Then, the graphene coverage parameter (ratio of the number of white pixels to the total number of pixels in the image expressed as a percentage) is calculated. The code also counts the number of individual zones in the image that are covered with graphene (each zone is made up of a set of pixels of the same color) and uses it to

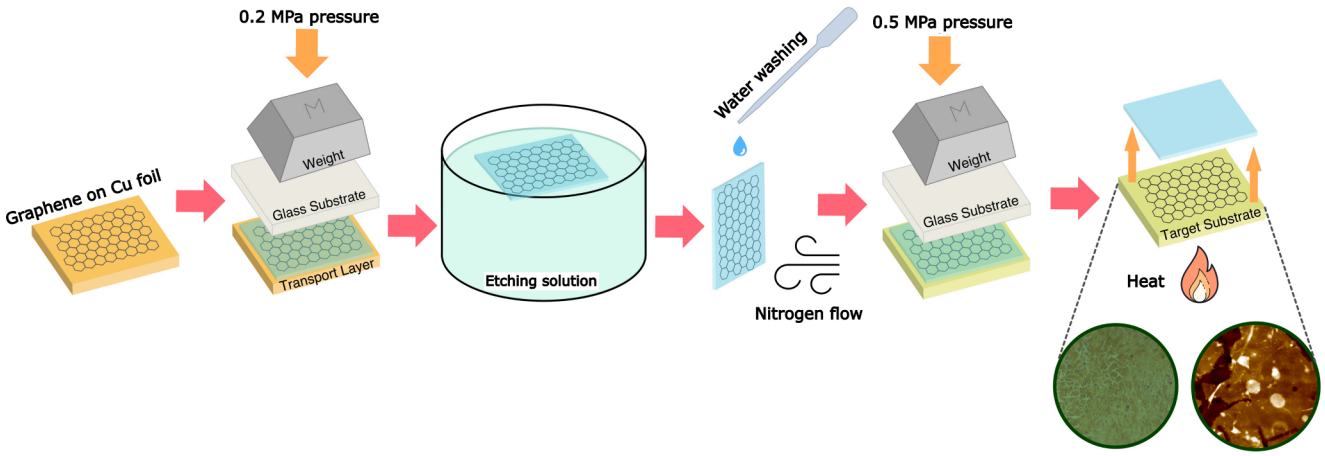

Scheme 1. Representation of PDMS- and TRT-assisted graphene transfer methods. Target substrate corresponds to Si/SiO_2 substrate.

calculate the uniformity parameter and a figure of merit (FoM) which gives a quantitative overall representation of the coverage and uniformity of the transferred graphene. The formulas used for calculating the uniformity parameter and the FoM correspond to Equation (1) and (2) respectively, which are defined by the authors of this work. A more detailed explanation of the operation of the code can be found in Section I of the supporting information document. The full code is available in a separate supporting document.

$$U = \frac{1}{(Z_i)^{0.25}} * 100 \tag{1}$$

$$FoM = \frac{C * U}{100} \tag{2}$$

In the equations, U is the uniformity parameter, Z_i corresponds to the individual zones (i.e., the individual areas that were not effectively covered with graphene after the transfer process), FoM is the figure of merit and C stands for the coverage. For calculating the residues parameter, the image of interest is binarized using a process analogous to that used when determining the coverage, so that white pixels correspond to residues instead of covered areas. Then, the ratio of the white pixels to the total pixels of the image is calculated and multiplied by 100 to express it as a percentage.

3. Results and discussion

3.1. Image analysis based on optical microscopy images

Full characterization of graphene, regardless of whether it has been subjected to a transfer process or not, has typically been done using Raman mapping. However, this technique poses the challenge of requiring equipment that is not readily available in many research facilities. This has motivated several studies aiming to make this process more low-cost oriented, e.g., using computer-based strategies [31–33].

Following this effort, here we present an alternative macroscopic characterization focused on the coverage, uniformity and amount of residues of transferred graphene. The characterization relies mainly on optical microscopy images, which are employed as input for MATLAB-based image analysis, thus making it easy to employ without the need for advanced and expensive equipment.

A detailed explanation of the operation of the MATLAB code used for the image analysis is shown in Section I of the Supplementary Information document. Shortly, the code works in the following way:

1. The image of interest is converted to grayscale to make it easier to binarize (conversion of the image to black and white).
2. The grayscale image is binarized using a preinstalled app in the Image Processing Toolbox available in the MATLAB library. Here, a tuning of the binarization process is required to make it reliable. This tuning depends on the substrate onto which the graphene was transferred, since the color gamut obtained in the microscopy images used for the analysis depends on it. Section II of the Supplementary Information document shows how the tuning process can be carried out.
3. After the binarization of the grayscale image, the areas covered with graphene in the image are assigned to white pixels, whereas the uncovered areas are assigned to black pixels. From this binarized image the coverage parameter is calculated by determining the ratio of white pixels to the total pixels of the image and multiplying it by 100 (to express it as a percentage).
4. Using the binarized image, the number of individual uncovered zones is determined. Each zone is made up of a set of black pixels, and by counting the number of individual sets in the image this value is obtained. Thereafter, Equation (1) is used to calculate the uniformity parameter of the image.

Equation (1) shows an inverse proportionality between the uniformity parameter (U) and the number of individual zones (Z_i). This is due to the nature of the equation employed for calculating the parameter, causing the appearance of a larger number of isolated areas that are not covered with graphene in the image to generate a lower value in the uniformity parameter. The isolated areas can be visualized as holes left by the transfer process, thus making it reasonable to obtain a less uniform transfer when more isolated areas are present. The equation can be tuned depending on how sensible it may be required to be to small changes in the number of individual zones in the analyzed images. Fig. 1a shows the dependance of the uniformity parameter on the number of individual zones when using different exponents in the equation (the value to which the number of individual zones is raised in Equation (1). It can be noticed that higher exponents make the uniformity parameter more sensitive to small changes in the number of individual zones. This can also be corroborated in Fig. 1b, where the difference between the value of the uniformity parameter corresponding to 1 (best case scenario) and 10 individual zones is shown as a function of the exponent. It can be noticed that higher exponents cause a larger difference in the values of the uniformity parameter. In this work, an exponent of 0.25 was used since it produced noticeable differences between "good" and "bad" transfer results during the optimization that was carried out to define the parameters used in the transfer methods shown in the methodology.

5. Finally, Equation (2) is used to calculate the FoM based on the previously binarized image. This parameter is used as an overall value

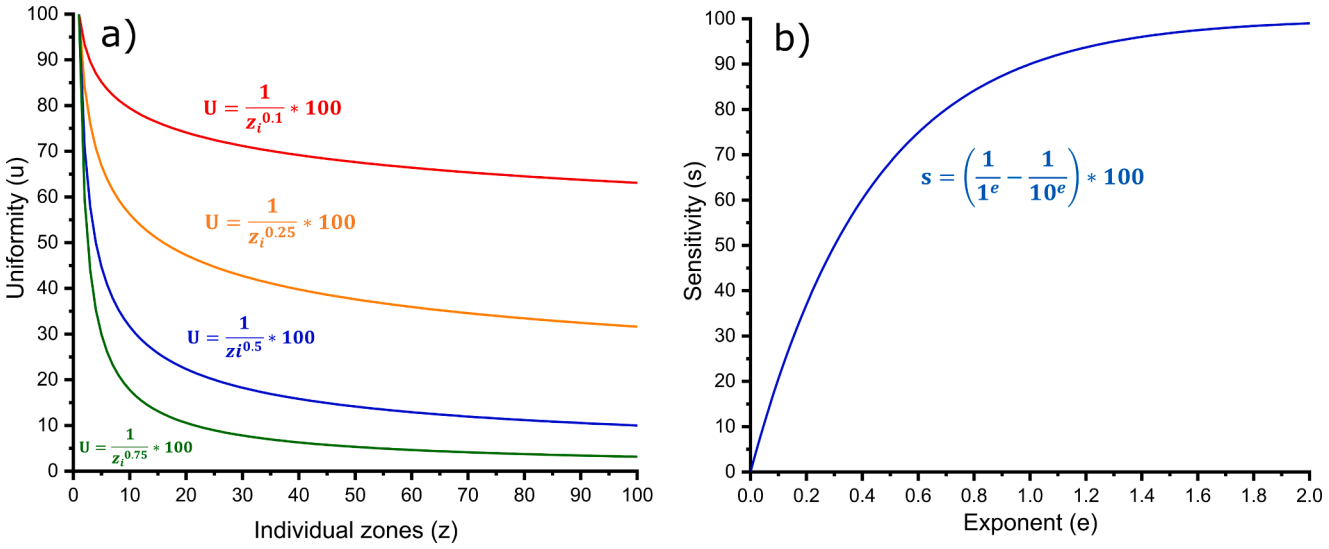

Fig. 1. A) Dependance of uniformity on the number of individual zones with different exponents, **b)** dependance of sensitivity on exponent.

that indicates the coverage and uniformity obtained after a graphene transfer process.

The code also calculates a residues parameter, which is a quantification of the residues left during the transfer process that are visible in the image. For this, the image of interest is binarized using a process analogous to that shown in step 3 (see Section I in Supplementary Information), so that white pixels correspond to residues instead of covered areas. In the case presented here, in which Si/SiO_2 was used as target substrate, the residues can be easily segmented by performing a binarization because they have a dark appearance once the image is converted to grayscale. The bulky shape of the residues left by the carrier substrate and the purple-like background color given by the Si/SiO_2 substrate in the optical microscopy images result in the residues having a greenish appearance, i.e., the pixels corresponding to the residues have a higher green value in the RGB color model. The function used by MATLAB to transform the image to grayscale uses a simple expression to assign an "intensity" value to each pixel in the grayscale based on their red, green a blue value, being the green the component with the highest coefficient in the equation, i.e., the one that contributes the most to the intensity of each pixel. This causes the dark appearance of the residues in the grayscale images that allows the segmentation to be easily performed (see Figure S1 for a comparison of the images before and after their conversion to grayscale).

The code operates on the defined images by the user, i.e., the process is carried out for each one of the optical microscopy images of interest. Afterwards, the parameters calculated from images corresponding to the same transfer process (the condition of interest) are averaged and the standard deviation is calculated for each one.

The code used in this work can be executed in a semi-automatic or automatic configuration. In the automatic, the analysis of each individual image is performed without considering errors that might occur during the binarization of the image, e.g., a very small zone made up of a set of black pixels could be considered as a not-covered individual zone when it is not (see Section I of the Supplementary Information document for more detail). When executed using the semi-automatic configuration, the code accounts for this type of errors by requesting the user to draw the smallest visible zone that is not covered with graphene in each image. This makes the analysis more extensive but also more reliable. Hence, we strongly recommend using the semi-automatic configuration.

It is important to note that the image analysis presented here does not serve as a full characterization of the transferred graphene per se. Instead, it focuses on the macroscopic physical features (coverage, uniformity, and presence of residues) which may be altered due to transfer process and are discernible from optical microscopy images of graphene on a target substrate. Thus, it can be used as an evaluation tool of the transfer process itself. Other features, including the number of layers of the graphene, and the appearance of structural disorder, must be evaluated with complementary techniques, e.g., Raman Spectroscopy, Raman Mapping and Atomic Force Microscopy. As a transfer process evaluation tool, the method can be significantly useful and practical when analyzing standardized transfer methods or optimizing them, especially when good coverage and uniformity is required. The automatization potential of this method and its non-dependance on costly equipment makes it highly compatible with industrial-scale processes, e.g., a large area can be studied making use of many images, whose acquisition can be automated, and proper calibration (see Section I and II of the Supplementary Information document).

Once the image analysis method was defined, it was employed to evaluate 3 transfer processes (PDMS-, TRT- and PMMA- assisted transfers onto Si/SiO_2 substrates) and make a direct comparison between them based on the calculated parameters. Additionally, the analysis was complemented by employing Raman spectroscopy to assess the number of layers and the structural disorder of the graphene before (on the copper foil) and after the different transfer processes (on the Si/SiO_2 substrates), thus allowing a better understanding of the effect of the transfer itself in the properties of graphene, e.g., the introduction of folds and structural disorder. Afterwards, a direct comparison using image analysis was made and its validity was confirmed by Raman mapping.

3.2. *Characterization of graphene on copper foil*

As a reference, the initial CVD-grown graphene on copper foil was characterized using SEM and Raman spectroscopy. Fig. 2a shows a SEM image of CVD-grown graphene on the copper foil used for the transfer process. The areas covered with graphene can be easily identified as darker gray regions. It is important to note that some well-defined small areas of the copper foil are not covered with graphene (lighter gray color in Fig. 2a), meaning that obtaining 100 % coverage in a transfer process is unfeasible. However, when disregarding these small areas, the areas that are effectively covered display high coverage. A value of 92 % was obtained for the coverage parameter in these areas when performing MATLAB-based image analysis on several SEM images (shown in Figure S6). This indicates that the maximum coverage that could be achieved after a transfer process must be near to this value. The small white zones that can be seen in the SEM images, some of which have a

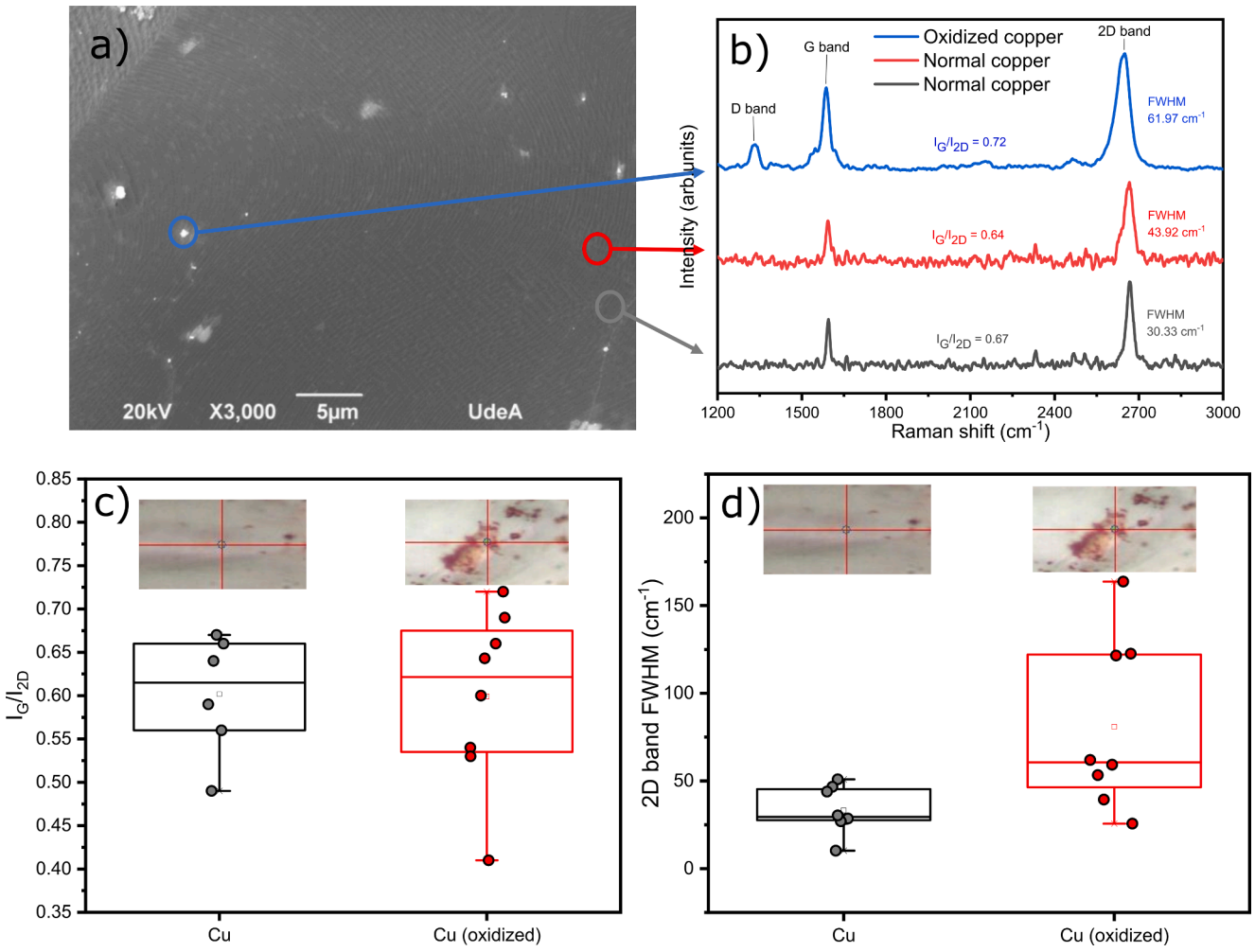

Fig. 2. a) SEM image of graphene on Cu foil (darker zones correspond to graphene), **b)** representative Raman spectra taken in different zones of CVD-grown graphene on copper foil. **c)** Intensity ratio IG/I2D and **d)** 2D band FWHM calculated from 14 Raman spectra taken from CVD-grown graphene on copper foil. The insets of the graphs show the representative area in which the spectra were taken.

particle-like shape (see Figure S6d), were identified as oxygen enriched areas, corresponding to oxidized copper based on EDS analysis (Figure S7).

Representative Raman spectra were taken in oxidized and not oxidized zones of the copper foil (all covered with graphene), which are shown in Fig. 2b. Fig. 2c and 2d show the I_G/I_{2D} ratio and Full Width at Half Maximum (FWHM) values of the 2D bands calculated from 14 Raman spectra taken in oxidized and not oxidized regions. The I_G/I_{2D} ratio (or its reciprocal) is a parameter that can be used to determine whether graphene is monolayer or multilayer, since its value changes depending on the number of layers [35]. Also, both the FWHM and the shape of the 2D band give valuable information about the number of layers of graphene in a sample since they also change depending on the number of layers [35–41]. The 2D band in monolayer graphene can be fitted to a single Lorentzian peak, which has been proven to be a reliable fitting for this band [36], while multilayer graphene displays a multi-peak structure related to the dispersion of π electrons during the Raman scattering process [37]. For instance, in the case of bilayer graphene, the 2D band can be fitted with 4 Lorentzian peaks, each of them corresponding to a different double resonance process during Raman scattering [37,42]. This causes the 2D band in multilayer graphene to display a higher FWHM than monolayer graphene.

According to Fig. 2, the zones with no oxidized copper display an I_G/I_{2D} ratio close to 0.5, and the FWHM values of the 2D bands lie between 30.33 and 43.92 cm^{-1}, which indicates that the CVD-grown corresponds to MLG [35]. The D band, sometimes observed in Raman spectra of graphene, is related to structural defects in this material. This band results from a first-order Raman process where a charge carrier is excited by incident light and inelastically scattered by a phonon. Then a second elastic scattering by a defect in the crystal lattice of graphene must occur to result in recombination [43,44]. These defects can be classified as zero-dimensional (0D) and one-dimensional (1D), and information about their presence and nature in a sample can be acquired from the D band. The former includes vacancies, dopants or functional chemical groups, while the latter includes dislocations and crystallite borders [38,45–47]. Therefore, the lack of a D band (usually appearing at about 1350 cm^{-1} depending on the energy of the laser used for the excitation due to its dispersive nature [48]) in the spectra obtained from non-oxidized zones indicates the absence of the aforementioned defects in the graphene hexagonal structure (or at least their presence is non-significant). On the other hand, Raman spectra obtained from the oxidized zones show a significant intensity of the D band (at 1334 cm^{-1}) thus causing the I_D/I_G ratio to be greater than zero, while the values of the I_G/I_{2D} ratio (0.72) and the FWHM of the 2D band (61.79 cm^{-1}) indicate that the graphene is not monolayer (NMG) [35,41]. Representative values showing the difference between the 2D band FWHM, I_G/I_{2D} and I_D/I_G ratio in oxidized and not oxidized zones of the copper foil are shown later in Table 1. Initially, graphene is grown on the surface of a pristine copper foil, meaning that the appearance of oxide on the copper surface occurs after some time of exposure to an oxygen-containing

Table 1
Representative values of 2D band FWHM, I_G/I_{2D} and I_D/I_G ratios acquired from Raman spectra from pristine graphene on copper foil and transferred graphene employing PDMS-, TRT- and PMMA-assisted processes.

Substrate/Transfer		I_G/I_{2D}	I_D/I_G	2D band FWHM (cm^{-1})
Copper	**Clean**	0.67	~0	30.33
	Oxidized	0.72	0.31	61.97
PDMS-assisted	**Clean**	0.67	0.19	35.17
	With residues	0.99	0.2	42.05
TRT-assisted	**Clean**	0.69	0.16	31.37
	With residues	0.92	0.49	43.09
PMMA-assisted	**Clean**	1.33	0.86	44.27
	With residues	1.34	0.47	44.14

atmosphere, which is likely to take place during the manipulation and storing of the copper foil. Therefore, the change from MLG to NMG on the copper foil might be caused by folding of the initially MLG layer occurring due to the mechanical deformation generated by changes in density when copper oxide is formed. However, the oxidized zones are scarce, indicating that the appearance of the D band, i.e., the introduction of structural defects in the structure, or other changes in the Raman spectrum of the graphene after the transfer process must be induced by the process itself.

3.3. Characterization of transferred graphene onto Si/SiO_2 substrates

Representative images of transferred graphene onto Si/SiO_2 substrates using each of the evaluated methods are show in Fig. 3a, 3b, 3c. Graphene transferred using the PMMA-assisted process (Fig. 3c) shows residues with a river-like appearance, whereas the residues from the PDMS- and TRT-assisted transfers display a more rounded shape. Section III of the supporting information shows details about the operation of the latter 2 substrates when used for graphene transfer processes. Representative Raman spectra from graphene transferred employing each method and their corresponding I_G/I_{2D} ratios are shown in Fig. 3d, 3e, 3f. The FWHM and the Lorentz-fitted curves of the 2D band of each spectrum are shown in Fig. 3g. All 2D bands could be fitted with a single Lorentzian peak, and the corresponding FWHM and I_G/I_{2D} ratios corroborate that the graphene is monolayer [35,36].

However, a more representative insight can be obtained by considering more Raman spectra taken from several points of the sample. Box plots showing the I_D/I_{2G} ratios and the FWHM values of the 2D band (calculated via a Lorentz peak fitting), obtained from over 15 Raman spectra taken from several points of the samples (both with and without residues) from each transfer process are shown in Fig. 4a and 4b, respectively. Data obtained from Raman spectra taken from zones with residues are indexed with the suffix -r in the x-axis labels of the box plots.

The I_G/I_{2D} ratios obtained in "clean" graphene (i.e., graphene with no residues) transferred using the TRT-assisted process ranged from 0.54 to 0.86 and the corresponding 2D band FWHM values from 29.67 to 36.35 cm^{-1}, indicating that all the analyzed zones correspond to MLG (in which 2D band FWHM values range from ~ 25 to 40 cm^{-1} [35]). In the case of the PDMS-assisted process, I_G/I_{2G} ratios and 2D band FWHM values obtained from "clean" graphene ranged from 0.62 to 0.94 and 32.65 to 46.82 cm^{-1}, respectively. This indicates that most of the transferred graphene is monolayer (10 out of the 12 spectra that were analyzed correspond to MLG). Only 2 of the analyzed zones displayed I_G/I_{2D} ratios (0.94 and 0.82) and 2D band FWHM values (46.82 and 44.7 cm^{-1}) that lay outside the monolayer graphene ranges [35,49]. Interestingly, in most of the spectra taken from zones with residues, both in TRT- and PDMS-assisted processes, the I_G/I_{2D} ratios approached a value of 1 and the 2D band FWHM values entered the bilayer graphene zone (in which 2D band FWHM values range from ~ 40 to 50 cm^{-1} [35]). This indicates that the residues left by the carrier substrates tend to fold the MLG that is being transferred, making it change into bilayer or multilayer graphene. Surprisingly, in the case of PMMA-assisted process the obtained I_G/I_{2D} ratios and FWHM values showed that most of the transferred graphene was bilayer or multilayer [35,49]. Furthermore, there were no significant differences between the "clean" graphene and the zones with residues, both being multilayer. This might be because the PMMA layer used to transfer the graphene from the copper foil to the Si/SiO_2 substrate was too thin, and while scooping it from the etching solution with the target substrate it was likely to unintentionally fold it, causing initially MLG to change into NMG during the transfer process itself.

As mentioned before, I_D/I_G ratio can be used to gain insight into the amount of structural defects, namely 0D and 1D defects, in graphene [38,47,50]. The I_D/I_G ratios calculated from Raman spectra of graphene transferred with TRT- and PDMS-assisted processes, both in "clean" zones and zones with residues, are shown in Figure S8 as box plots. Table 1 also shows representative values of the I_D/I_G ratios in these cases. When comparing the I_D/I_G values obtained in the PDMS- and TRT-assisted transfer processes, the ones corresponding to the latter are the lowest, indicating that this method (TRT-assisted) introduces the least amount of structural defects in the graphene structure. However, the zones with residues in this process (indexed as TRT r in the x-axis of the box plot shown in Figure S8) show higher values of I_D/I_G, implying that in this case the residues cause the graphene to have more structural defects. This might be related to the folding that was proposed to occur based on the changes observed in the I_G/I_{2D} ratios between zones with and without residues. On the other hand, no significant differences were

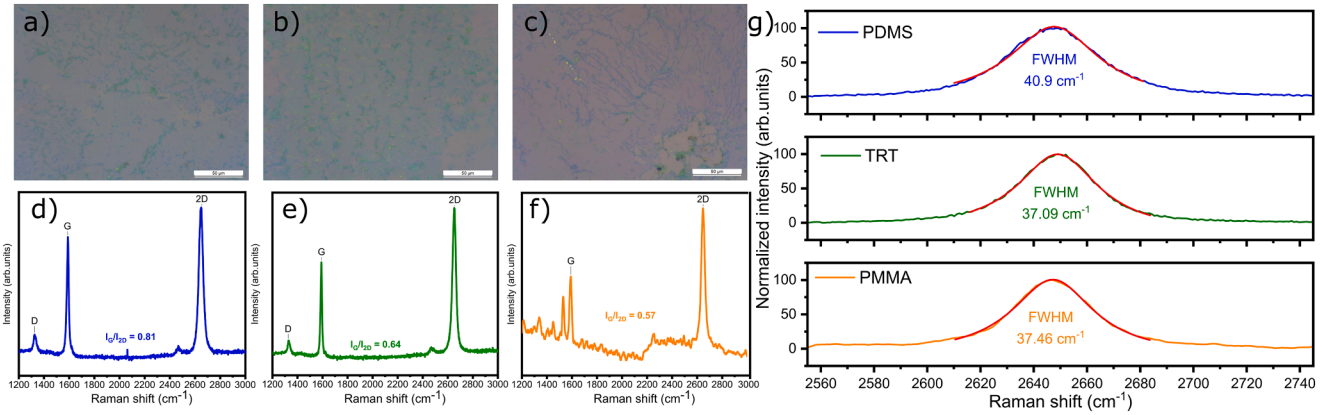

Fig. 3. Optical microscopy images taken at 500x zoom of graphene on Si/SiO_2 substrate transferred with **a)** PDMS, **b)** TRT, **c)** PMMA and representative Raman spectra taken from graphene transferred with **d)** PDMS, **e)** TRT and **f)** PMMA. g) Lorentz fitting of 2D band taken from several Raman spectra of graphene transferred using several transfer substrates.

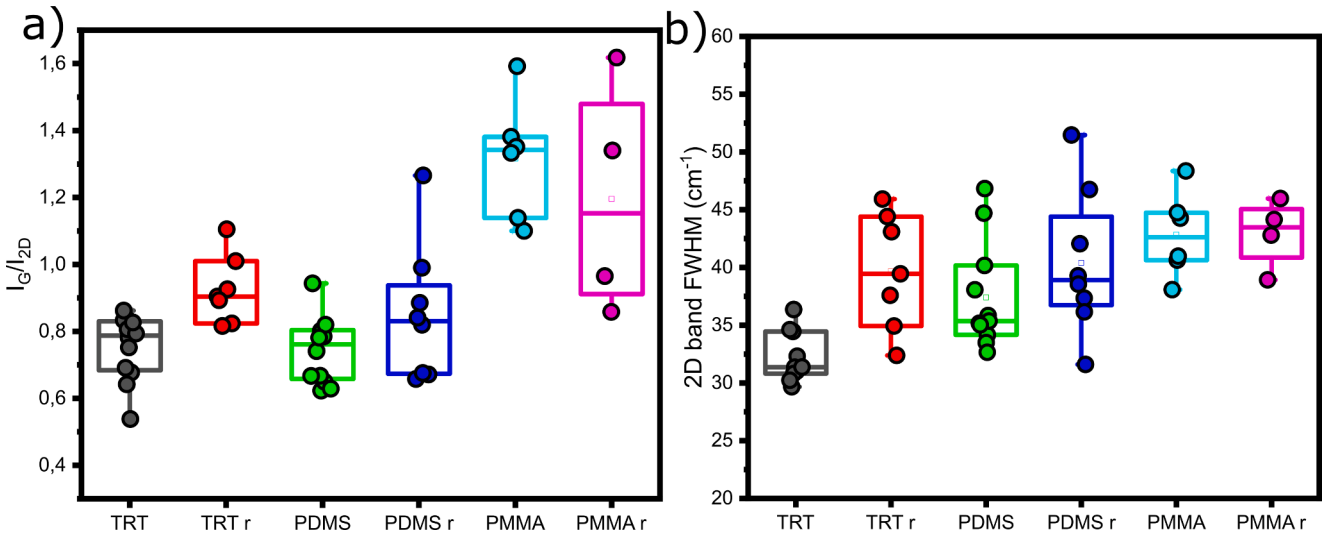

Fig. 4. **a)** Comparison of I_G/I_{2D} ratios and **b)** 2D band FWHM calculated from Raman spectra obtained in "clean" graphene zones and zones with residues (r) for the 3 evaluated transfer methods.

observed between the clean zones and the ones with residues in the case of PDMS-assisted transfer process, which points to the fact that the change from MLG to NMG caused by the residues does not introduce further defects in the structure.

Furthermore, in the case of PDMS- and TRT-assisted processes, where the transferred graphene is MLG (zones without residues), more information about the nature of the defects introduced in the structure by the transfer process itself can be gained by analyzing the areas of the D and G bands (A_D and A_G respectively) as well as the FWHM value of the G band. We estimated the density of 0D and 1D defects (σ_D and σ_A respectively) in two different zones of the graphene transferred under these conditions based on the method introduced by Cançado et. al and the results are shown in Table S1 [47]. In both PDMS- and TRT-assisted transfers the density of 1D defects is significantly higher than the density of 0D defects (the difference is more than two orders of magnitude), although they can vary between different zones in the same transferred graphene. This shows that the structural defects introduced during these transfer processes causing the appearance of the D band in the Raman spectra are mostly 1D.

3.4. Image analysis of transferred graphene onto Si/SiO_2 substrates

Image analysis performed using the MATLAB code designed by the authors was employed for evaluating the 3 graphene transfer processes on Si/SiO_2 substrates (PDMS-, TRT- and PMMA-assisted), for which optical microscopy images of the as-transferred graphene taken at 500x were used. This is because lower magnifications did not allow small empty zones (zones without transferred graphene) to be effectively observed. The transferred area of the graphene on the substrates was approximately 25 mm^2. The analysis was performed using different amounts of images and it was noticed that there were no significant differences between the results obtained using 10, 20, 30 and 40 images (see Figure S9), meaning that the analyzed area in each transfer was highly uniform. This is likely to be due to the transferred area being small by itself, making it less probable to find meaningful differences between the values calculated for the parameters from one region to another, i.e., from one image to another. Thus, using 10 images (corresponding to a ratio of 0.4 images per mm^2 of transferred graphene) is sufficient to obtain representative results in this case.

Fig. 5 and Table 2 show the parameters calculated for each transfer process. The average coverage values obtained for the PMMA-, TRT- and PDMS-assisted transfer processes were 85.19, 85.17 and 82.46 % respectively. Thus, coverages exceeding 80 % were obtained in all cases

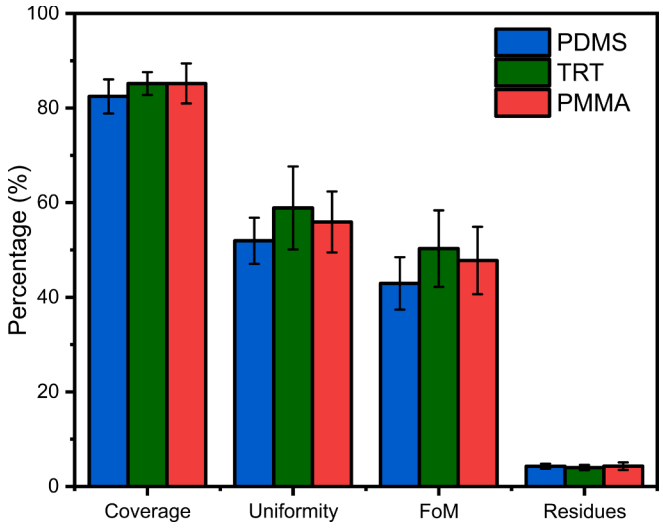

Fig. 5. Transfer parameters calculated for each transfer method. 10 images of each transfer method were used for the calculation.

and both the standard PMMA- and TRT-assisted processes displayed the best results in this regard. The main difference was observed in the uniformity values of the processes, where average values of 55.91, 58.88 and 51.94 % were obtained for the PMMA-, TRT- and PDMS-assisted processes, respectively. The TRT-assisted process showed the best results in this regard, thus yielding the best value for the FoM (50.29 %). On the other hand, the average FoM values obtained for the PMMA- and PDMS-assisted transfer processes were 47.77 and 42.94 %, respectively. The TRT-assisted process also displayed the least amount of residues (4 %), although all three processes showed very low and similar values of this parameter (4.31 and 4.28 % for PMMA- and PDMS-assisted).

These parameters, particularly the FoM, offer a direct way of reliably comparing two or more graphene transfer processes based on the coverage, uniformity and amount of residues that can be observed in it. Moreover, these parameters were readily calculated from mere optical microscopy images, which can be obtained routinely and automatically, using a MATLAB code and no expensive equipment was used for the actual calculation of the previously stated parameters. This shows the ease of use of the evaluation method and its low-cost and industry-compatible operation. For verifying the validity of the proposed

Table 2
Average calculated transfer parameters for PDMS-, TRT- and PMMA-assisted transfer processes with standard deviation. *STD: Standard deviation.

Transfer process	Coverage (%)		Uniformity (%)		FoM (%)		Residues (%)	
	Mean	STD*	Mean	STD	Mean	STD	Mean	STD
PDMS-assisted	82.46	3.61	51.94	4.87	42.94	5.54	4.28	0.52
TRT-assisted	85.17	2.42	58.88	8.76	50.29	8.09	4	0.56
PMMA-assisted	85.19	4.23	55.91	6.45	47.77	7.13	4.31	0.79

method, graphene transferred using PDMS- and TRT-assisted processes was characterized via Raman mapping (see Section V of the Supporting Information document). The coverages calculated using this technique are in good agreement with the results obtained using the MATLAB-based image analysis method, demonstrating its validity. Furthermore, the code proved to be useful when using different target substrates, i.e., Si/SiO_2 substrates and ITO-coated glass substrates, showing that the main requirement for the code to operate properly is that visible contrast between the areas that are covered with graphene and the ones that are not exists. This is the case for both target substrates that were evaluated. More information on the use of the code when employing ITO-coated glass substrates as target can be found in Section VI of the supplementary information document.

4. Conclusions

In summary, the MATLAB-based image analysis method presented in this works allows a simple and reliable evaluation of graphene transfer processes based on the macroscopic coverage, uniformity, and residues discernible in optical microscopy images of graphene on the target substrate, which was corroborated by employing it to compare 3 different transfer processes carried onto Si/SiO_2 substrates and also validated for ITO-coated glass substrates. In this way, it was demonstrated that a quantitative comparison between several transfer processes or transfer conditions can be readily performed by employing a method which is non-dependent on costly characterization equipment and whose operation is straightforward, low-cost oriented and industry compatible. The method can also be applied to graphene transferred onto different target substrates when a previous calibration of the code in terms of the commands used to binarize the optical microscopy images of the transferred graphene is done. For this, a total of 4 parameters defined by the authors (coverage, uniformity, residues, and a Figure of Merit which is calculated using the first 2) were used to effectively quantify the aforementioned features of the transferred graphene. The method was complemented by employing Raman spectroscopy to evaluate the number of layers and the structural disorder of the graphene before and after the different transfer processes, which allowed a better understanding of the effect of the transfer itself on the properties of graphene. When comparing the evaluated transfer processes, a coverage surpassing 80 % was observed in each case, being the average values for the PMMA-, TRT- and PDMS- assisted processes 85.19, 85.17 and 82.46 % respectively (in the case of graphene transferred onto ITO-coated glass, the average coverage was 79.94 %). However, the image analysis clearly showed that the best result is obtained using the TRT-assisted transfer method, since it yielded the highest FoM (50.29 %), the lowest value of the residues parameter (4 %) and fewer defects were induced in the graphene crystal structure, as revealed by Raman Spectroscopy. This indicates that, regarding the coverage and uniformity of the transferred graphene, this method might be the most suitable one for applications where these features are important. Furthermore, the results obtained using the image analysis were in good agreement with results obtained using Raman Mapping, demonstrating its validity.

CRediT authorship contribution statement

Kevin Ballestas: Investigation, Data curation, Writing – original draft. **Juan Diego Zapata:** Conceptualization, Methodology, Resources, Writing – review & editing. **Daniel Ramírez:** Conceptualization, Methodology, Resources, Writing – review & editing.

Declaration of Competing Interest

The authors declare the following financial interests/personal relationships which may be considered as potential competing interests: [Daniel Ramirez reports financial support was provided by Colombia Ministry of Science Technology and Innovation. Juan D. Zapata reports financial support was provided by University of Antioquia].

Data availability

Data will be made available on request.

Acknowledgements

The authors would like to thank Minciencias for the financial support of this work under contract 177-2021, and Fundación Universidad de Antioquia– FUA from Universidad de Antioquia (G8-2020 1108 39306, 2022-55290). UdeA 2023-58610.

Appendix A. Supplementary data

Supplementary data to this article can be found online at https://doi.org/10.1016/j.apsusc.2023.158074.

References

[1] K.S. Novoselov, A.K. Geim, S.V. Morozov, D. Jiang, Y. Zhang, S.V. Dubonos, I. V. Grigorieva, A.A. Firsov, Electric field effect in atomically thin carbon films, Science 80 (306) (2004) 666–669, https://doi.org/10.1126/science.1102896.
[2] K.S. Novoselov, A.K. Geim, S.V. Morozov, D. Jiang, M.I. Katsnelson, I. V. Grigorieva, S.V. Dubonos, A.A. Firsov, Two-dimensional gas of massless dirac fermions in graphene, Nature 438 (2005) 197–200, https://doi.org/10.1038/nature04233.
[3] H.I. Rasool, C. Ophus, W.S. Klug, A. Zettl, J.K. Gimzewski, Measurement of the intrinsic strength of crystalline and polycrystalline graphene, Nat. Commun. 4 (2013) 1–7, https://doi.org/10.1038/ncomms3811.
[4] P. Zhang, L. Ma, F. Fan, Z. Zeng, C. Peng, P.E. Loya, Z. Liu, Y. Gong, J. Zhang, X. Zhang, P.M. Ajayan, T. Zhu, J. Lou, Fracture toughness of graphene, Nat. Commun. 5 (2014) 1–7, https://doi.org/10.1038/ncomms4782.
[5] E.P. Randviir, D.A.C. Brownson, C.E. Banks, A decade of graphene research: Production, applications and outlook, Mater. Today. 17 (2014) 426–432, https://doi.org/10.1016/j.mattod.2014.06.001.
[6] B.R. Shivankar, C. Pratap, S. Krishnamurty, Applied Surface Science Chemically modified graphene sheets as potential sensors for organophosphate compounds (pesticide): A DFT study, Appl. Surf. Sci. 619 (2023) 156745, https://doi.org/10.1016/j.apsusc.2023.156745.
[7] D. Gao, S. Rao, Y. Li, N. Liu, D. Wang, Applied Surface Science Enhancement of CO adsorption energy on defective graphene-supported Cu 13 cluster and prediction with an induction energy model, Appl. Surf. Sci. 615 (2023) 156368, https://doi.org/10.1016/j.apsusc.2023.156368.
[8] S. Wu, K. Chiu, C. Fan, H. Chen, Applied Surface Science Electrocatalytic carbon dioxide reduction on graphene-supported Ni cluster and its hydride : Insight from first-principles calculations, Appl. Surf. Sci. 629 (2023) 157418, https://doi.org/10.1016/j.apsusc.2023.157418.
[9] M. Srivastava, A. Srivastava, Applied Surface Science Cu decorated functionalized graphene for Arsenic sensing in water : A first principles analysis, Appl. Surf. Sci. 560 (2021) 149700, https://doi.org/10.1016/j.apsusc.2021.149700.
[10] J.D. Zapata, D. Steinberg, L.A.M. Saito, R.E.P. De Oliveira, A.M. Cárdenas, E.A. T. De Souza, Efficient graphene saturable absorbers on D-shaped optical fiber for ultrashort pulse generation, Sci. Rep. 6 (2016) 1–8, https://doi.org/10.1038/srep20644.
[11] J.D. Zapata, L.A.M. Saito, A.M. Cárdenas, E.A.T. de Souza, Sub-150 fs mode-locked Erbium doped fiber laser based on monolayer graphene on a D-shaped optical

fiber, in: Conf. Lasers Electro-Optics, Optica Publishing Group, 2016: p. JTu5A.71. https://opg.optica.org/abstract.cfm?URI=CLEO_SI-2016-JTu5A.71.
[12] P.R. Somani, S.P. Somani, M. Umeno, Planer nano-graphenes from camphor by CVD, Chem. Phys. Lett. 430 (2006) 56–59, https://doi.org/10.1016/j.cplett.2006.06.081.
[13] L.P. Ma, W. Ren, H.M. Cheng, Transfer methods of graphene from metal substrates: A review, Small Methods. 3 (2019) 1–13, https://doi.org/10.1002/smtd.201900049.
[14] A. Reina, H. Son, L. Jiao, B. Fan, M.S. Dresselhaus, Z.F. Liu, J. Kong, Transferring and identification of single- and few-layer graphene on arbitrary substrates, J. Phys. Chem. C. 112 (2008) 17741–17744, https://doi.org/10.1021/jp807380s.
[15] H.H. Kim, S.K. Lee, S.G. Lee, E. Lee, K. Cho, Wetting-assisted crack- and wrinkle-free transfer of wafer-scale graphene onto arbitrary substrates over a wide range of surface energies, Adv. Funct. Mater. 26 (2016) 2070–2077, https://doi.org/10.1002/adfm.201504551.
[16] X. Li, Y. Zhu, W. Cai, M. Borysiak, B. Han, D. Chen, R.D. Piner, L. Colomba, R. S. Ruoff, Transfer of large-area graphene films for high-performance transparent conductive electrodes, Nano Lett. 9 (2009) 4359–4363, https://doi.org/10.1021/nl902623y.
[17] X. Liang, B.A. Sperling, I. Calizo, G. Cheng, C.A. Hacker, Q. Zhang, Y. Obeng, K. Yan, H. Peng, Q. Li, X. Zhu, H. Yuan, A.R. Hight Walker, Z. Liu, L.M. Peng, C. A. Richter, Toward clean and crackless transfer of graphene, ACS Nano 5 (2011) 9144–9153, https://doi.org/10.1021/nn203377t.
[18] S. Bae, H. Kim, Y. Lee, X. Xu, J.S. Park, Y. Zheng, J. Balakrishnan, T. Lei, H. Ri Kim, Y. Il Song, Y.J. Kim, K.S. Kim, B. Özyilmaz, J.H. Ahn, B.H. Hong, S. Iijima, Roll-to-roll production of 30-inch graphene films for transparent electrodes, Nat. Nanotechnol. 5 (2010) 574–578, https://doi.org/10.1038/nnano.2010.132.
[19] J. Kang, S. Hwang, J.H. Kim, M.H. Kim, J. Ryu, S.J. Seo, B.H. Hong, M.K. Kim, J. B. Choi, Efficient transfer of large-area graphene films onto rigid substrates by hot pressing, ACS Nano 6 (2012) 5360–5365, https://doi.org/10.1021/nn301207d.
[20] B. Jang, C.H. Kim, S.T. Choi, K.S. Kim, K.S. Kim, H.J. Lee, S. Cho, J.H. Ahn, J. H. Kim, Damage mitigation in roll-to-roll transfer of CVD-graphene to flexible substrates, 2D Mater. 4 (2017), https://doi.org/10.1088/2053-1583/aa57fa.
[21] Y. Lee, S. Bae, H. Jang, S. Jang, S.E. Zhu, S.H. Sim, Y. Il Song, B.H. Hong, J.H. Ahn, Wafer-scale synthesis and transfer of graphene films, Nano Lett. 10 (2010) 490–493, https://doi.org/10.1021/nl903272n.
[22] T. Choi, S.J. Kim, S. Park, T.Y. Hwang, Y. Jeon, B.H. Hong, Roll-to-roll continuous patterning and transfer of graphene via dispersive adhesion, Nanoscale 7 (2015) 7138–7142, https://doi.org/10.1039/c4nr06991a.
[23] J.L.P. Morin, N. Dubey, F.E.D. Decroix, E.K. Luong-Van, A.H.C. Neto, V. Rosa, Graphene transfer to 3-dimensional surfaces: A vacuum-assisted dry transfer method, 2D Mater. 4 (2017), https://doi.org/10.1088/2053-1583/aa6530.
[24] S.Y. Yang, J.G. Oh, D.Y. Jung, H.K. Choi, C.H. Yu, J. Shin, C.G. Choi, B.J. Cho, S. Y. Choi, Metal-etching-free direct delamination and transfer of single-layer graphene with a high degree of freedom, Small 11 (2015) 175–181, https://doi.org/10.1002/smll.201401196.
[25] L. Banszerus, M. Schmitz, S. Engels, J. Dauber, M. Oellers, F. Haupt, K. Watanabe, T. Taniguchi, B. Beschoten, C. Stampfer, Ultrahigh-mobility graphene devices from chemical vapor deposition on reusable copper, Sci. Adv. 1 (2015) 1–7, https://doi.org/10.1126/sciadv.1500222.
[26] X. Wang, J. Zhang, X. Zhang, Y. Zhu, Characterization, uniformity and photo-catalytic properties of graphene/TiO_2 nanocomposites via Raman mapping, Opt. Express. 25 (2017) 21496, https://doi.org/10.1364/oe.25.021496.
[27] J.D. Buron, D.H. Petersen, P. Bøggild, D.G. Cooke, M. Hilke, J. Sun, E. Whiteway, P. F. Nielsen, O. Hansen, A. Yurgens, P.U. Jepsen, Graphene conductance uniformity mapping, Nano Lett. 12 (2012) 5074–5081, https://doi.org/10.1021/nl301551a.
[28] D.M.A. Mackenzie, J.D. Buron, P.R. Whelan, J.M. Caridad, M. Bjergfelt, B. Luo, A. Shivayogimath, A.L. Smitshuysen, J.D. Thomsen, T.J. Booth, L. Gammelgaard, J. Zultak, B.S. Jessen, P. Bøggild, D.H. Petersen, Quality assessment of graphene: Continuity, uniformity, and accuracy of mobility measurements, Nano Res. 10 (2017) 3596–3605, https://doi.org/10.1007/s12274-017-1570-y.
[29] B.N. Chandrashekar, A.S. Smitha, Y. Wu, N. Cai, Y. Li, Z. Huang, W. Wang, R. Shi, J. Wang, S. Liu, S. Krishnaveni, F. Wang, C. Cheng, A universal stamping method of graphene transfer for conducting flexible and transparent polymers, Sci. Rep. 9 (2019) 1–11, https://doi.org/10.1038/s41598-019-40408-w.
[30] Y. Sheng, Y. Rong, Z. He, Y. Fan, J.H. Warner, Uniformity of large-area bilayer graphene grown by chemical vapor deposition, Nanotechnology 26 (2015), https://doi.org/10.1088/0957-4484/26/39/395601.
[31] C.M. Nolen, G. Denina, D. Teweldebrhan, B. Bhanu, A.A. Balandin, High-throughput large-area automated identification and quality control of graphene and few-layer graphene films, ACS Nano 5 (2011) 914–922, https://doi.org/10.1021/nn102107b.
[32] Y. Saito, K. Shin, K. Terayama, S. Desai, M. Onga, Y. Nakagawa, Y.M. Itahashi, Y. Iwasa, M. Yamada, K. Tsuda, Deep-learning-based quality filtering of mechanically exfoliated 2D crystals, Npj Comput. Mater. 5 (2019) 1–6, https://doi.org/10.1038/s41524-019-0262-4.
[33] X. Dong, H. Li, Z. Jiang, T. Grünleitner, I. Güler, J. Dong, K. Wang, M.H. Köhler, M. Jakobi, B.H. Menze, A.K. Yetisen, I.D. Sharp, A.V. Stier, J.J. Finley, A.W. Koch, 3D deep learning enables accurate layer mapping of 2D materials, ACS Nano 15 (2021) 3139–3151, https://doi.org/10.1021/acsnano.0c09685.
[34] N. Villa, J.D. Zapata, D. Ramirez, Paraffin wax assisted chemical vapor deposited graphene transfer method, Thin Solid Films 721 (2021) 138556, https://doi.org/10.1016/j.tsf.2021.138556.
[35] Y. Wang, S.W. Tong, X.F. Xu, B. Özyilmaz, K.P. Loh, Interface engineering of layer-by-layer stacked graphene anodes for high-performance organic solar cells, Adv. Mater. 23 (2011) 1514–1518, https://doi.org/10.1002/adma.201003673.
[36] L.M. Malard, M.A. Pimenta, G. Dresselhaus, M.S. Dresselhaus, Raman spectroscopy in graphene, Phys. Rep. 473 (2009) 51–87, https://doi.org/10.1016/j.physrep.2009.02.003.
[37] L.G. Cançado, A. Reina, J. Kong, M.S. Dresselhaus, Geometrical approach for the study of G′ band in the raman spectrum of monolayer graphene, bilayer graphene, and bulk graphite, Phys. Rev. B - Condens. Matter Mater. Phys. 77 (2008) 1–9, https://doi.org/10.1103/PhysRevB.77.245408.
[38] A. Das, B. Chakraborty, A.K. Sood, Raman spectroscopy of graphene on different substrates and influence of defects, Bull. Mater. Sci. 31 (2008) 579–584, https://doi.org/10.1007/s12034-008-0090-5.
[39] Y. Hao, Y. Wang, L. Wang, Z. Ni, Z. Wang, R. Wang, C.K. Koo, Z. Shen, J.T. L. Thong, Probing layer number and stacking order of few-layer graphene by Raman Spectroscopy, Small 6 (2010) 195–200, https://doi.org/10.1002/smll.200901173.
[40] J.S. Park, A. Reina, R. Saito, J. Kong, G. Dresselhaus, M.S. Dresselhaus, G′ band Raman spectra of single, double and triple layer graphene, Carbon N. Y. 47 (2009) 1303–1310, https://doi.org/10.1016/j.carbon.2009.01.009.
[41] A.C. Ferrari, J.C. Meyer, V. Scardaci, C. Casiraghi, M. Lazzeri, F. Mauri, S. Piscanec, D. Jiang, K.S. Novoselov, S. Roth, A.K. Geim, Raman Spectrum of Graphene and Graphene Layers 187401 (2006) 1–4, https://doi.org/10.1103/PhysRevLett.97.187401.
[42] L.M. Malard, J. Nilsson, D.C. Elias, J.C. Brant, F. Plentz, E.S. Alves, A.H. Castro Neto, M.A. Pimenta, Probing the electronic structure of bilayer graphene by Raman scattering, Phys. Rev. B - Condens. Matter Mater. Phys. 76 (2007) 1–4, https://doi.org/10.1103/PhysRevB.76.201401.
[43] I. Childres, L. Jauregui, W. Park, H. Caoa, Y.P. Chena, Raman spectroscopy of graphene and related materials, new dev. phot, Mater. Res. (2013) 403–418.
[44] C. Thomsen, S. Reich, Double resonant raman scattering in graphite, Phys. Rev. Lett. 85 (2000) 5214–5217, https://doi.org/10.1103/PhysRevLett.85.5214.
[45] Y. You, Z. Ni, T. Yu, Z. Shen, Edge chirality determination of graphene by raman spectroscopy, Appl. Phys. Lett. 93 (2008) 2006–2009, https://doi.org/10.1063/1.3005599.
[46] T. Xu, L. Sun, Structural defects in graphene, defects adv, Electron. Mater. Nov. Low Dimens. Struct. 5 (2018) 137–160, https://doi.org/10.1016/B978-0-08-102053-1.00005-3.
[47] L.G. Cançado, M.G. Da Silva, E.H. Martins Ferreira, F. Hof, K. Kampioti, K. Huang, A. Pénicaud, C.A. Achete, R.B. Capaz, A. Jorio, Disentangling contributions of point and line defects in the Raman spectra of graphene-related materials, 2D Mater. 4 (2017), https://doi.org/10.1088/2053-1583/aa5e77.
[48] R. Saito, M. Hofmann, G. Dresselhaus, A. Jorio, M.S. Dresselhaus, Raman spectroscopy of graphene and carbon nanotubes, Adv. Phys. 60 (2011) 413–550, https://doi.org/10.1080/00018732.2011.582251.
[49] H.G. Rosa, J.A. Castañeda, C.H.B. Cruz, L.A. Padilha, J.C.V. Gomes, E.A. Thoroh de Souza, H.L. Fragnito, Controlled stacking of graphene monolayer saturable absorbers for ultrashort pulse generation in erbium-doped fiber lasers, Opt. Mater. Express. 7 (2017) 2528, https://doi.org/10.1364/ome.7.002528.
[50] M. Castriota, G.G. Politano, C. Vena, M.P. De Santo, G. Desiderio, M. Davoli, E. Cazzanelli, C. Versace, Variable angle spectroscopic ellipsometry investigation of CVD-grown monolayer graphene, Appl. Surf. Sci. 467–468 (2019) 213–220, https://doi.org/10.1016/j.apsusc.2018.10.161.